International Journal of Smart Sensor and Adhoc Network

Volume 3 | Issue 1 Article 8

October 2012

SLOT LOADED SHORTED GAP COUPLED BROADBAND MICROSTRIP ANTENNA

SARTHAK SINGHAL
Department of Electronics Engineering,IIT(BHU),Varanasi, ssinghal@gmail.com

SLOT LOADED SHORTED GAP COUPLED BROADBAND MICROSTRIP ANTENNA

SARTHAK SINGHAL

Department of Electronics Engineering,IIT(BHU),Varanasi

Abstract- In this paper the bandwidth of a conventional rectangular microstrip antenna has been enhanced by locating capacitively excited $\lambda_m/4$ short circuit parasitic elements at its radiating and non-radiating edges along with the circular polarization and loading the parasitic elements with the rectangular slots. An impedance bandwidth of 1.53513 GHz to 1.843438 GHz (308.3MHz). It has three resonances at 1.56GHz, 1.67GHz and 1.8 GHz. The result are simulated by MOM based IE3D software.

Index Terms- *Circular polarization, non-radiating edges, radiating edges, RMSA.*

I. INTRODUCTION

Microstrip antennas are receiving much attention owing to their advantages of having low profile, light weight, simple and inexpensive to manufacture and printed-circuit-construction. They are finding applications in aircraft, satellite, wireless and mobile communication. For linearly polarized microstrip antennas, the bandwidth is limited by variations of the input impedance and a commonly used definition for bandwidth is the frequency range over which input voltage standing wave ratio (VSWR) is less than two. The major disadvantages of the microstrip antenna are narrow bandwidth and low frequency. Among the many forms of RMSA developed, the most useful form is open circuit patch antenna [1-2]. It has a disadvantage of bandwidth of the order of 1% only at frequencies of 1-2GHz.

The bandwidth of open circuited printed antenna can be enhanced by using the substrate of lesser dielectric constant or the thicker substrate whereas the exact shape of the patch does not have a dominant effect on the bandwidth if the overall dimensions are similar. It can also be increased by introducing capacitively excited $\lambda_m/4$ parasitic elements located at their radiating and non-radiating edges. The BW and beamwidth can be further improved by shorting the edges of the parasitic elements.

In the present paper, the bandwidth has been enhanced by introducing slots on the parasitic patches gap-coupled to the radiating and non-radiating edges of the central patch. The proposed antenna design is simulated by using MOM based IE3D software.

II. ANTENNA DESIGN

The configuration of the proposed antenna is in a symmetrical outline. It supports two modes like those of $\lambda_m/2$ open-circuit patch with two parasitic elements one oriented along each axis. Two equal modes were excited due to the feed location on the central patch diagonal. The antenna structure gets circularly polarized due to the presence of the central slot which acts as an inductive loading resulting into detuning of one of the modes.

The geometry of the proposed antenna along with its dimensions is shown in Figure1. It has been designed on a substrate having h=3.18mm, ε_r=2.5 and tan δ=0.001 and a size of 10.6 mm X 10.6 mm. The central square patch having dimensions of (51mm X 51mm) is loaded with a central slot of dimensions (25.5mm X 2mm). The parasitic patches having dimensions of (52mm X 25.5mm) are located at a gap of 2mm from the edges of the central patch. The central patch is fed by a coaxial probe of diameter 1.2 mm along its principle diagonal at the location of (14.75mm, 14.75mm). The parasitic elements have been shorted along their edges by a shorting wall. The shorting wall has been implemented by an arrangement of shorting pins of diameter of 1.59mm and separated by a distance of 6mm.

The lengths of the slots on parasitic elements are varied to find the optimum solution while keeping the feed location fixed. The width of the slots on parasitic elements is fixed at 1mm.

III. METHOD OF ANALYSIS

The use of thicker substrates results in undesirable spurious radiations and the dielectric constant cannot be reduced below a limit value practically. So the bandwidth is increased by using gap coupled parasitic patches. In general, microstrip antennas are linearly polarized causing support for one mode only. To further increase the bandwidth, circular polarization is introduced which supports two equal modes of $\lambda_m/2$ open circuit patch with two parasitic elements, one oriented along each axis. The short circuits are placed at the edges of the parasitic patches to reduce the size of the antenna required for such a large bandwidth. In [3], a similar configuration is analyzed.

In the presented work, the bandwidth has been further enhanced by using the slots in parasitic patches.

IE3D is the first SCALABLE EM design and verification plate form that delivers the modeling accuracy for the combined needs of high frequency circuit design and signal integrity engineers across multiple design domains. It is based on method of moments (MOM). IE3D's multi-threaded and distributed simulation architecture and high-design capacity is the most cost-effective EM simulation and modeling solution for component-level and circuit-level applications. IE3D offers the highest simulation capacities and fastest turnaround times for the broadest number of applications making it the best choice for improving your design team productivity and meeting design schedules on time.

IV. RESULTS AND DISCUSSION

During the parametric analysis of the proposed antenna, the length of the shorting wall along the edges of the parasitic elements is varied from one-fourth to the full shorting wall and it is observed that the optimum bandwidth is obtained for full shorting wall length. From Fig. 2 and Table 1, bandwidth of 249.1MHz with resonance frequencies of 1.67 GHz and 1.8 GHz was obtained for full length of shorting wall.

After optimizing the shorting wall length, the parasitic elements are loaded with slots of fixed width and variable length. The length of the slots on parasitic elements along the y-axis and x-axis is varied by keeping the length of the slots on the parasitic elements lying along another axis fixed.

From VSWR and return loss variation, shown in Fig. 3(a) and Fig. 3(b) respectively and Table 2, it is observed that on varying the slot length (y) from 18.75 mm to 22 mm the bandwidth increases from 290MHz to 309.8MHz. The resonance frequencies of 1.56GHz, 1.67GHz and 1.8 GHz are unaffected whereas the overall percentage bandwidth varies from 17.26190 to 18.44048.

From VSWR and return loss variation, shown in Figure 3(c) and Figure 3(d) respectively and Table 3, it can be observed that on increasing the slot length (x) from 2.75 mm to 12.75mm the resonances are unaffected whereas the bandwidth decreases resulting into variation of the overall percentage bandwidth from 18.31548 to 17.27381.

The real and imaginary parts of the input impedance are shown in Figure 3(e). It can be seen that for the operating range the real part is varying from 68.7 Ω to 139 Ω whereas the imaginary part varies between 112 Ω to -31 Ω. From the smith chart plot shown in Fig. 3(f), it can be seen that the impedance loci has two loops in the VSWR=2 circle. It shows the same result as shown by Figure 3(b) and Figure 3(d).

The optimum solution is found for slot lengths of x=0mm and y=21.75mm on parasitic elements. It has three resonances at frequencies of 1.56GHz, 1.67GHz and 1.8GHz along with a bandwidth of 308.3MHz and f_o=1.68GHz.

The simulated total field directivity versus frequency plot is shown in Figure 4.The radiation pattern for the antenna with all equal resonators at both resonance frequencies of 1.56GHz, 1.67 GHz and 1.8GHz is calculated at $\varphi=0^0$ and $\varphi=90^0$ for both E and H-plane. The radiation patterns are shown in Figure 5.

The 3D radiation patterns and the current distribution for the proposed antenna design at three resonance frequencies are shown in Figure 6 and Figure 7 respectively.

TABLE 1. VSWR, RESONANCE FREQUENCY AND BANDWIDTH WITH FULL SHORTING WALL LENGTH

RES	f_{O1}(GHz)	f_{O2}(GHz)	VSWR at f_{O1}	VSWR at f_{O2}	BW (MHz)
FULL	1.67	1.8	1.30973	1.26077	249.1

Table 2. Bandwidth Variation With Various Parasitic Slot Length(y) With Fixed Slot Width at1mm

SLOT LENGTH, x (mm)	SLOT LENGTH, y (mm)	BW [MHz, %]
0	18.75	290.00, 17.26190
0	21.00	303.22, 18.04881
0	21.50	306.60, 18.25000
0	21.70	308.00, 18.33333
0	21.75	308.30, 18.35119
0	22.00	309.80, 18.44048

Table 3. Bandwidth Variation With Various Parasitic Slot Length(x) With Fixed Slot Width at 1mm

SLOT LENGTH, x (mm)	SLOT LENGTH, y (mm)	BW[MHz,%]
2.75	21.75	307.70,18.31548
4.75	21.75	306.50,18.24405
6.75	21.75	304.50,18.12500
8.75	21.75	300.40,17.88095
10.75	21.75	297.00,17.67857
12.75	21.75	290.20,17.27381

V. CONCLUSION

According to the results obtained on simulating the proposed antenna designed we can conclude that the bandwidth is heavily dependent on the length of the slots on the parasitic elements coupled to the non-radiating edges. Due to wider beamwidth this antenna can be used for short distance communication system like television receivers, terrestrial Eureka 147 digital audio broadcasting, military use, GNSS, telecommunication etc.

ACKNOWLEDGEMENT

Sarthak Singhal is very thankful to the Ministry of Human Resources and Development for providing me the financial assistance in the form of GATE scholarship.

REFERENCES

[1] Munson, R.E.: 'Conformal microstrip antennas and microstrip phased arrays'. IEEE Trans, 1974, AP-22, pp.74-78

[2] HOWELL, J.Q.: 'Microstrip Antennas', ibid, 1975, AP-23, pp. 90-93

[3] C.Wood, "Improved bandwidth of microstrip antennas using parasitic elements", IEEE PROC, Vol. 127, Pt. H, No. 4, August 1980, pp 231- 234

[4] G.Kumar and K.C.Gupta," Broad-Band Microstrip Antennas Using Additional Resonators Gap-Coupled to the Radiating Edges", IEEE Transactions on antennas and propagation, vol. Ap-32, no. 12, December 1984, pp.1375-1379,

[5] Kerr, J.: 'Microstrip antenna developments', Proceedings of workshop on printed circuit antenna technology, New Mexico State University, October 1979, pp. 3. 1-3. 20

[6] IE3D 14.1, Zeland Software Inc., Fremont, CA, 2008

[7] I.J. Bahl and P. Bhartia, Microstrip antennas, Artech House, Norwood, MA, 1980.

[8] G. Kumar and K.P. Ray, Broadband Microstrip Antennas, Artech House, Norwood, MA, 2003.

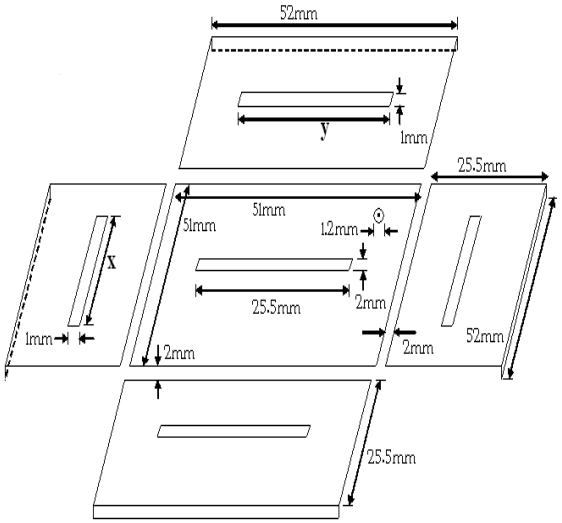

Figure 1 Configuration of the proposed antenna structure

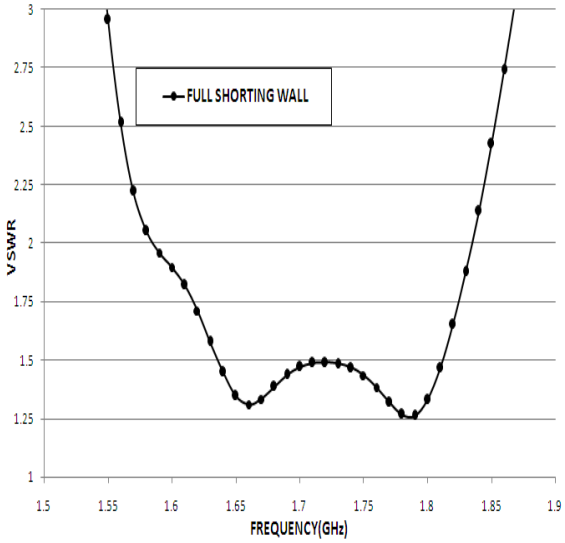

Figure 2 VSWR versus frequency plot for full length of shorting wall

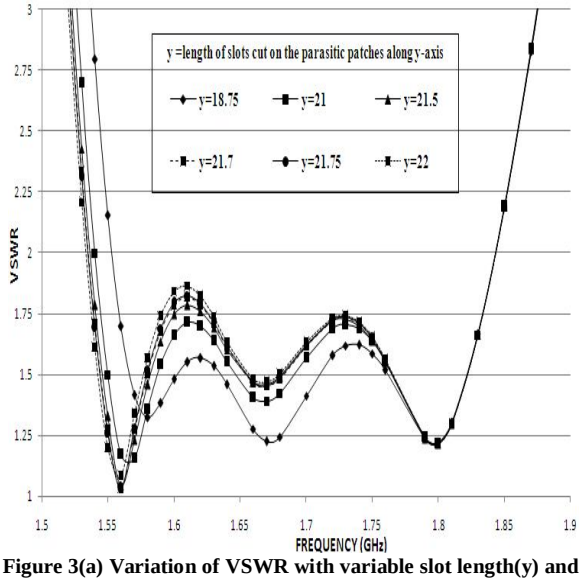

Figure 3(a) Variation of VSWR with variable slot length(y) and fixed slot length(x=0mm)

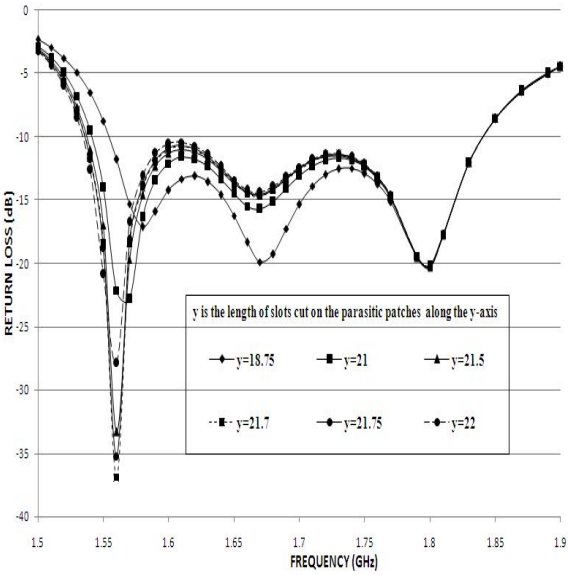

Figure 3(b) Variation of return loss with variable slot length(y) and fixed slot length(x=0mm)

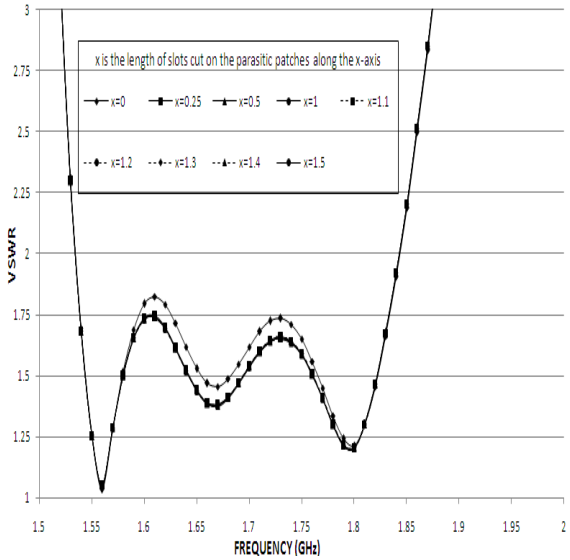

Figure 3(c) Variation of VSWR with variable slot length(x) and fixed slot length(y=21.75mm)

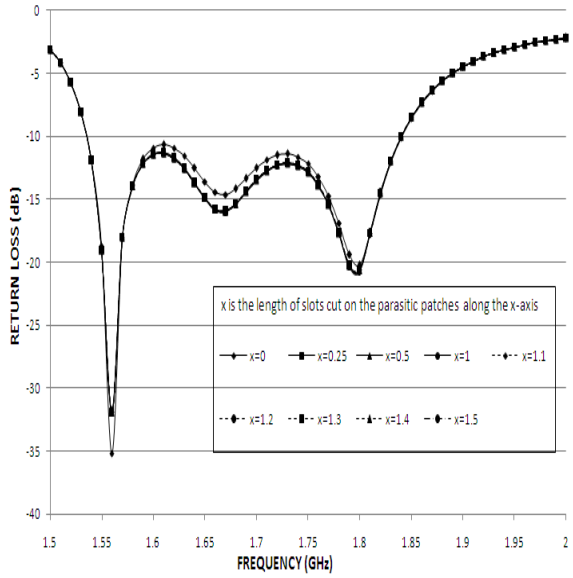

Figure 3(d) Variation of return loss with variable slot length(x) and fixed slot length(y=21.75mm)

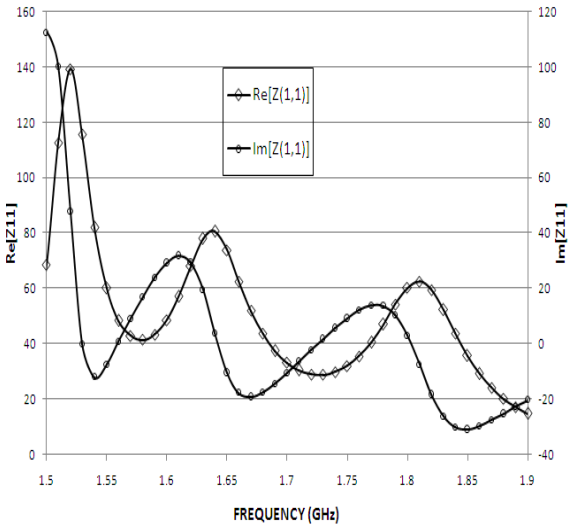

Figure 4(e) Simulated input impedance plot for the proposed antenna design with x=0mm and y=21.75mm

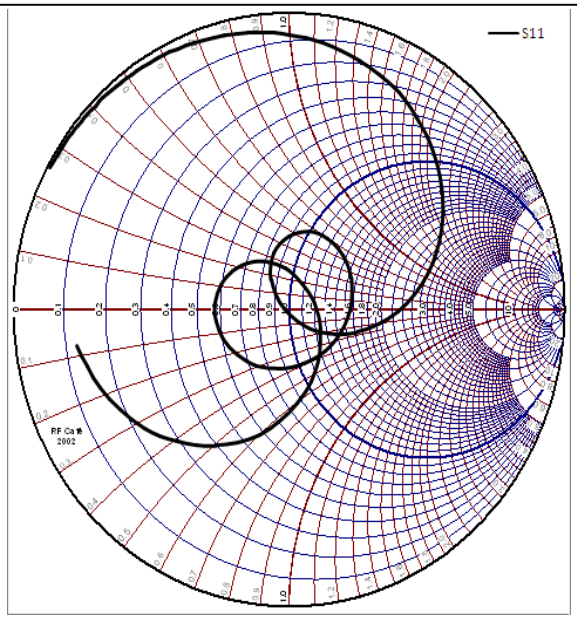

Figure 5(f) Simulated Smith chart plot for the proposed antenna design with x=0mm and y=21.75mm

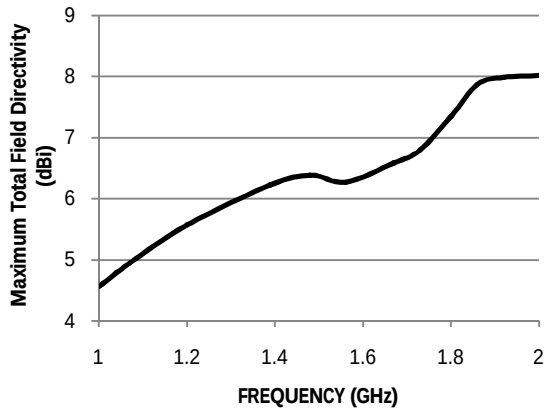

Figure 4 Simulated Maximum Total Field Directivity versus frequency plot for the proposed antenna design

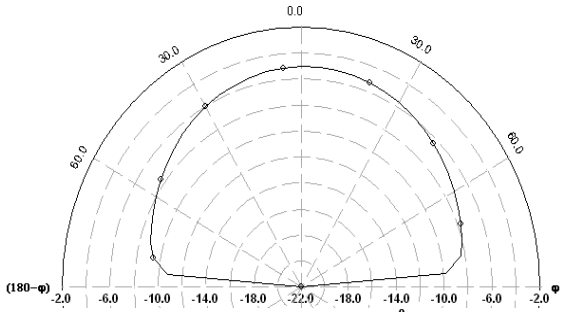

Figure 5(a) Radiation pattern of E_θ at $\Phi = 0^0$ for f_0=1.56 GHz

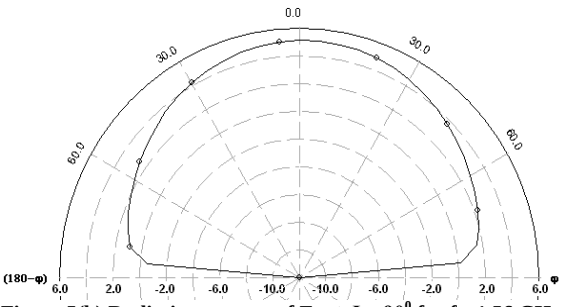

Figure 5(b) Radiation pattern of E_θ at $\Phi = 90^0$ for f_0=1.56 GHz

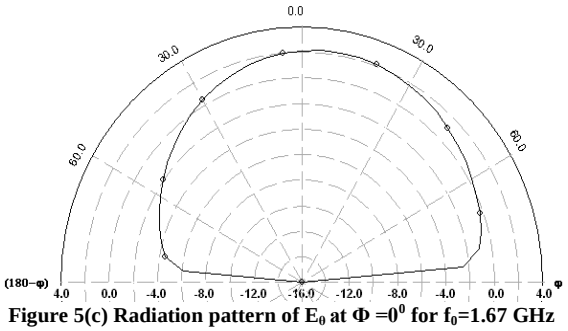

Figure 5(c) Radiation pattern of E_θ at $\Phi = 0^0$ for f_0=1.67 GHz

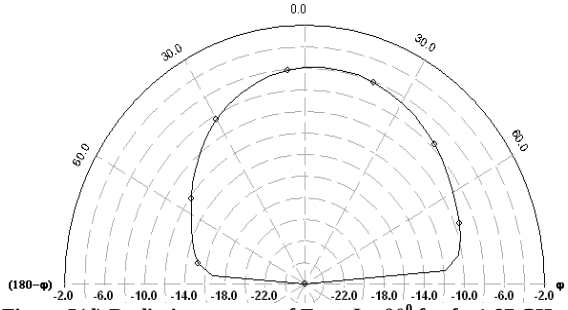

Figure 5(d) Radiation pattern of E_θ at $\Phi = 90^0$ for f_0=1.67 GHz

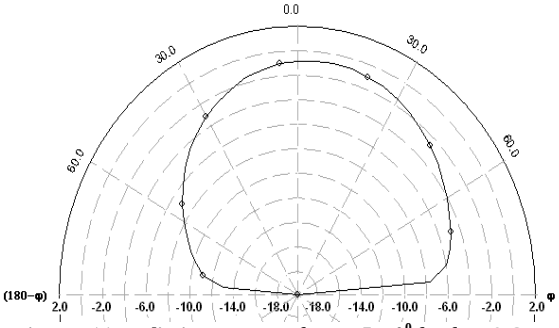

Figure 5(e) Radiation pattern of E_θ at $\Phi = 0^0$ for f_0=1.8 GHz

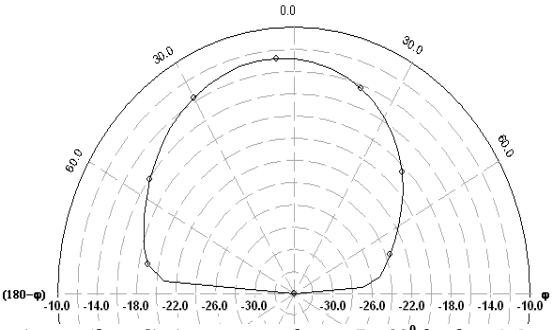

Figure 5(f) Radiation pattern of E_θ at $\Phi = 90^0$ for f_0=1.8 GHz

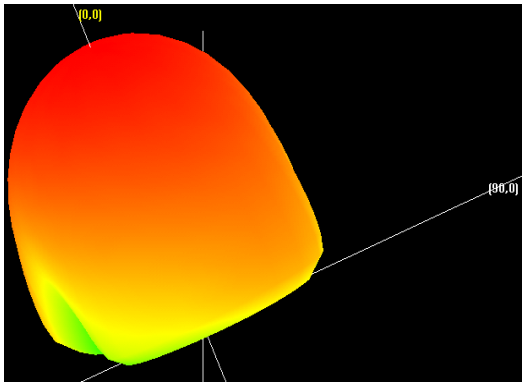

Figure 6(a)3D Radiation pattern at f_0=1.56 GHz

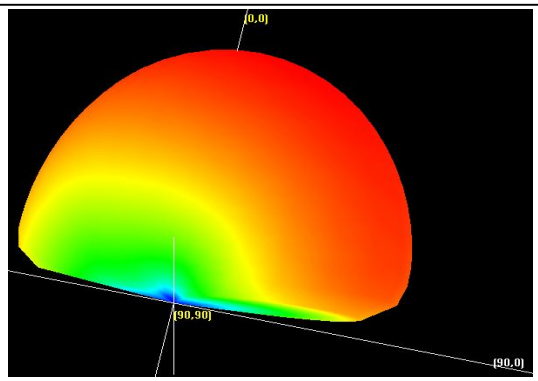

Figure 6(b) 3D Radiation pattern at f_0=1.67 GHz

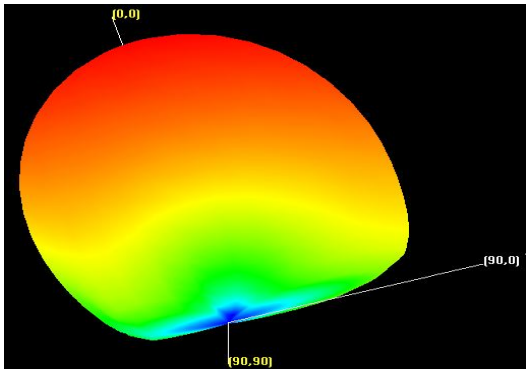

Figure 6(c) 3D Radiation pattern at f_0=1.80 GHz

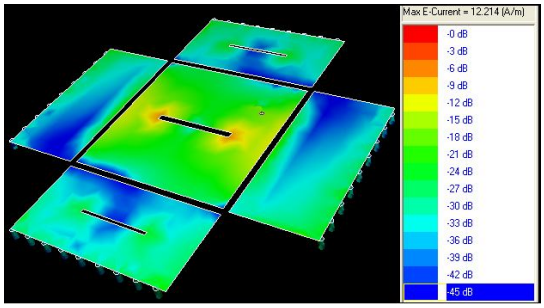

Figure 7(a) Current distribution at f_0=1.56 GHz

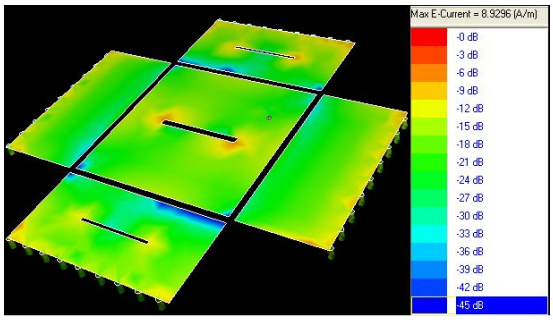

Figure 7(b) Current distribution at f_0=1.67 GHz

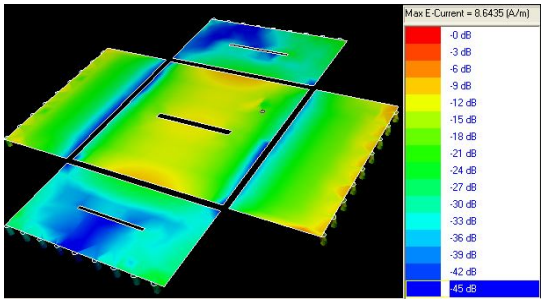

Figure 7(c) Current distribution at f_0=1.8 GHz